How are Large Western Hemisphere Warm Pools Formed?

David B. Enfield[1], Sang-ki Lee[2] and Chunzai Wang[1]

[1] NOAA Atlantic Oceanographic and Meteorological Laboratory, Miami, FL, 33149
[2] Cooperative Institute for Marine & Atmospheric Studies, Miami, FL, 33149

Submitted to *Journal of Climate*

October 2004

ABSTRACT

During the boreal summer the Western Hemisphere warm pool (WHWP) stretches from the eastern North Pacific to the tropical North Atlantic and is a key feature of the climate of the Americas and Africa. In the summers following nine El Niño events from 1950-2000, there have been five instances of extraordinarily large warm pools averaging about twice the climatological annual size. These large warm pools induced a strengthened divergent circulation aloft and have been associated with rainfall anomalies throughout the western hemisphere tropics and subtropics. However, following four other El Niño events large warm pools did not develop, such that the mere existence of El Niño during the boreal winter does not provide the basis for predicting a large warm pool the following summer.

In this paper we find consistency with the hypothesis that large warm pools result from an anomalous divergent circulation and weakened Atlantic Hadley cell, forced by sea surface temperature (SST) anomalies in the Pacific, i.e., the so-called atmospheric bridge. We also find significant explanations for why large warm pools do not always develop. If the El Niño event ends early, the Indo-Pacific warm pool anomaly lacks the persistence needed to force the atmospheric bridge and the Atlantic portion of the warm pool remains normal. If SST anomalies in the eastern Pacific do not last much beyond February of the following year, then the eastern North Pacific portion of the warm pool remains normal. The overall strength of the Pacific El Niño does not appear to be a critical factor. We also find that when conditions favor a developing atmospheric bridge and the winter atmosphere over the North Atlantic conforms to a negative NAO pattern (as in 1957-58 and 1968-69), the forcing is reinforced and the warm pool is stronger. On the other hand, if a positive NAO pattern develops the warm pool may remain normal even if other circumstances favor the atmospheric bride, as in 1991-92. Finally, we could find no evidence that interactions within the tropical Atlantic variability (TAV) are likely to mitigate for or against the formation of a large warm pool.

1. Introduction

The Western Hemisphere warm pool (WHWP) undergoes a very large annual variation in its geographic extent, almost disappearing in the boreal winter while extending from the eastern North Pacific into the tropical North Atlantic in late summer (Wang and Enfield 2001; Wang and Enfield 2003). For the purposes of this paper, the WHWP and its index can be defined as the area of sea surface temperature (SST) warmer than 28.5°C, including the eastern North Pacific (ENP) and the Intra-Americas Sea (IAS, including the Gulf of Mexico and Caribbean) extending eastward into the tropical North Atlantic (TNA, east of the Caribbean approximately between 5°N and 25°N) but not including the equatorial Atlantic (EQA) warm pool that develops in the boreal spring. Other isotherm definitions can be used (28.0°C, 27.5°C) but then the IAS and EQA portions merge during some months and make separation difficult. Inclusion of the EQA is inadvisable for this paper because its thermodynamics are different and its impact on Central and North American climates are not as clear. Inclusion of the ENP, however, is very important because it is part of the total SST heating signal (including the IAS) that the atmosphere sees north of the equator in the boreal summer when the WHWP becomes the heating focus for the divergent circulation for the Americas sector of the troposphere.

Year-to-year variations in warm pool size can be quite large, with the largest anomalies being comparable to the yearly mean size. A 1950-2000 time series of the WHWP area index (Figure 1a) is well correlated ($r = 0.60$) with the index of sea surface temperature in the TNA (Figure 1d) (Wang and Enfield 2001). More interestingly, we see that the five largest warm pools (1958, 1969, 1983, 1987, 1998)

have occurred during the boreal summers following El Niño events and that these also correspond to some of the warmest years for the TNA, in agreement with Enfield and Mayer (1997). Note, however, that four other El Niño events in the record (1966, 1973, 1977, 1992) are not associated with large warm pools. Because large warm pools do not occur invariably as El Niño decays, the mere fact that an El Niño is in progress does not constitute an adequate basis for predicting a large warm pool during the following summer, nor the climate impacts attendant on large warm pools. It appears, therefore, that some factor affecting the aftermath of El Niño events may hold the key to predicting large warm pools and a warm TNA, which in turn influence much of the surrounding summer climates (Enfield 1996) long after the direct influence of El Niño on the winter climate has abated. The aim of this paper is to shed light on the processes that produce large warm pools following El Niño, and on the possible reasons for the failure of that mechanism under some circumstances.

Figures 1b,c show the component area indices for the ENP and IAS portions of the WHWP. In all of the five summers with large warm pools following El Niño peaks, the ENP portion had a large area. This is not surprising since the eastern Pacific frequently has significant SST anomalies (SSTA) that persist well into the second year of an El Niño event. However, in four of those years the IAS portion was also very large but those anomalies cannot be explained through a direct oceanic connection. Therefore, to understand the largest warm pool variations we must also understand how the warm pool-correlated TNA is affected by El Niño.

Enfield and Mayer (1997) and others have shown that interannual warmings of the TNA region west of West Africa following El Niño responds to a decrease in the

strength of the NE trade winds and associated latent heat loss and entrainment, with a consequent increase in the surface heat flux retained by the ocean mixed layer. Using primarily surface and satellite data, Klein et al. (1999) confirmed that the reduction of latent heat loss is the primary warming factor, but further showed that an increase in shortwave radiation due to reduced cloudiness constitutes a secondary, reinforcing influence. The largest part of the warm pool lies to the west of the TNA. But, while the TNA warming mechanisms may not apply equally to the warm pool core, the TNA warming alone can account for much of the increase in the area of the warm pool as defined by the 28.5°C, 28.0°C, or 27.5°C isotherms.

Klein et al. (1999) argue that both evaporation and solar radiation (cloud cover) are involved in the atmospheric bridge linking the oceans and that the relative importance of these and the seasonality of the remote forcing vary between regions. Using upper air fields from the NCAR/NCEP reanalysis (Kalnay et al. 1996), Hastenrath (2000) proposes that tropospheric subsidence over the subtropical North Atlantic is associated with reduced high pressure center at the surface (Hastenrath 1979) and the weakened trade winds responsible for the North Atlantic SST increase. He attributes this forcing to a train of pressure centers emanating from the Pacific across North America, i.e., the Pacific North American (PNA) pattern (Wallace and Gutzler 1981). In this paper we present a modified concept of the atmospheric bridge, similar to that discussed by Wang and Enfield (2003), and explore the possibility that for certain El Niño events the bridge does not develop to a significant degree, and/or that some external influence, such as the North Atlantic Oscillation (NAO) interferes with normal development of

the bridge. Either of these mechanisms could conceivably explain why large warm pools do not occur following all El Niño events.

After describing our data sources (section 2), in section 3 we outline our hypothesis for the atmospheric bridge and in sections 4 we use composite-average oceanic and atmospheric fields to demonstrate how the warm pool development differs between two sets of El Niño episodes: those with ensuing large warm pools and those without. In section 5 we consider the possibility that an external influences unrelated to El Niño — the North Atlantic Oscillation (NAO) and/or tropical Atlantic feedback processes— may also influence the effectiveness of the tropospheric bridge. In section 6 we discuss and summarize our results.

2. Data and methods

Our analyses rely primarily on various monthly averaged fields of the NCAR/NCEP atmospheric reanalysis (Kalnay et al. 1996), 1950-2000, including: SST; surface atmospheric pressure and winds; surface net heat flux, radiative and turbulent surface heat fluxes; 850 and 200 hPa velocity potential and irrotational wind; 500 hPa vertical velocity; 925 hPa pressure height and vector wind. To calculate the WHWP and TNA indices (Figure 1) we have used the 2° by 2° reconstructed SST data of Smith et al. (1996). For seasonal averaged and composite maps of SST anomaly we have used the NCEP/NCAR reanalysis data. For the NAO index we use the difference between normalized surface pressures at Lisbon Portugal and Reykjavik Iceland, 1864-1998 (Hurrell 1995).

Anomalies are formed by subtracting the 1950-2000 climatologies from the monthly fields but no other data treatments (smoothing, etc.) have been applied in preparing

seasonal averaged or composite maps. Surface flux anomalies are taken to be positive if they warm the ocean.

3. The atmospheric bridge of mature El Niño events

In this paper we prefer an alternate hypothesis (to Hastenrath 2000) regarding the atmospheric bridge, namely that the anomalous subtropical subsidence in the North Atlantic results directly through the tropical divergent circulation to the south (Walker and Hadley cell anomalies) rather than through a more circuitous PNA wave train to the north. The PNA pattern as documented with data by Wallace and Gutzler (1981) represents a series of covarying nodes in the tropospheric pressure height distributions, one of them being the negative node over the subtropical North Atlantic, which concerns us here. But there is nothing in the data to indicate that these nodes are necessarily linked through a wave-train phenomenon, notwithstanding the theoretical proposition of Hoskins and Karoly (1981) that they represent a standing Rossby wave in the atmosphere. Conversely, however, data for the divergent circulation (velocity potential and irrotational wind) show a clear link between the North Atlantic node of the PNA and the regional Hadley cell anomaly to the south (Figure 2).

The climatological mean winter divergent circulation of the upper troposphere (200 hPa) features a prominent outflow west of the dateline, over the Indo-Pacific warm pool (Figure 2a); convergence appears over the eastern equatorial Pacific and a second outflow occurs over northern South America. During El Niño winters, however, because of the strong thermal anomaly in the Pacific and the associated eastward expansion of the Indo-Pacific warm pool, the divergent circulation of the troposphere is strongly affected (Figure 2b). Anomalous convergence (divergence) appears west (east)

of the dateline, indicating that the outflow center has migrated eastward along with the eastward warm pool expansion below. As part of the altered Walker and Hadley circulations, the strength of convection and 200 hPa divergence over the Amazon Basin are decreased, thus weakening the northward outflow from there into the subtropical North Atlantic. The decreased subsidence over the North Atlantic subtropical high pressure system appears as a northeastward extension of the anomalous divergence over the eastern Pacific. The consequent decrease in subsidence near 25°-30°N in the Atlantic (Figure 2c) leads to a weakening of the North Atlantic subtropical high pressure system and a decrease in the NE trade winds (Enfield and Mayer 1997). This is, therefore, the hypothesis we have chosen to guide our analysis.

4. Evolution of large warm pools

In Figure 1a we see that 1958, 1969, 1983, 1987 and 1998 are all years with large warm pools. Each of these is the second year in a two-year sequence, the first year (0) being the El Niño onset phase and the second year (+1) being the decay phase of the event (Rasmusson and Carpenter 1982). Typically, the peak of the equatorial heating anomalies in the eastern Pacific occurs around November-December of the onset year (Enfield 1989). The group of biennia with large warm pools includes two very strong events (1982-83, 1997-98), one strong event (1957-58), and two weak-to-moderate events (1968-69, 1986-87) (Quinn and Neal 1992; Quinn et al. 1987). In each case we see that the summer of the second year has a warm pool ranging from 70% to 120% larger than the climatological July warm pool size.

In contrast, there appears to be no clear pattern for the size of the warm pool during the previous summers (onset years); they are near normal on average and they vary

between negative and positive anomalies. The only onset year with a large warm pool was 1997, which was entirely due to the ENP (Figure 1b) with no contribution from the Atlantic side (Figure 1c). In the early months of onset years the anomaly of the Indo-Pacific warm pool is small or negligible and not expected to impact the divergent circulation in a significant way, and therefore cannot create the conditions required in the Atlantic for a large Atlantic warm pool by early summer. Atlantic warm pool developments during the onset year are therefore mainly subject to atmosphere-ocean variability internal to the Atlantic sector and not correlated to El Niño.

Large warm pools do not follow a second group of widely recognized El Niño events, the (+1) years being 1966, 1973, 1977, and 1992 (Figure 1a). This group includes one strong event (1972-73) and three weak-to-moderate events (1965-66, 1976-77 and 1991-92) (Quinn and Neal 1992; Quinn et al. 1987). That this group is comprised of predominantly weaker El Niño events than in the first group suggests that the Pacific El Niño characteristics, such as intensity or timing, are a primary factor influencing the tropospheric forcing. However, the strong 1972-73 event (normal warm pool) does not fit this pattern as also the weak 1968-69 episode (large warm pool). An alternate or supplementary hypothesis is that some external factor, such as the North Atlantic Oscillation, reinforces or interferes with the development of the atmospheric bridge. In this section we explore the first hypothesis.

In Figures 1b, c we show the separate area indices for the ENP and IAS portions of the total warm pool. It is clear that both contribute to large warm pool anomalies and are correlated with the total warm pool index (r = 0.80, 0.85; lag = -1, 0 months) and with the tropical North Atlantic SSTA index (r = 0.42, 0.49; lags = 0 months)

(Figure 1). The rest of this section deals primarily with the remote forcing of the Atlantic portion of the warm pool. The role of the ENP portion will be discussed in the following section.

a. Composite evolution of SSTA

In Figure 3 we show the composite-averaged SSTA evolutions for the two sets of El Niño episodes: those followed by large warm pools (*WP*) on the left, and those not (*wp*), on the right. The first panel of each group shows the average SSTA distribution for November-December-January (NDJ), centered on December of year (0) when the Pacific equatorial cold tongue anomaly is usually maximum. The second panel is shown for the January-April (JFMA) period of year (+1). This four-month period is the one during which the resulting tropospheric anomalies noted by Klein et al. (1999) are persistent and force the tropical North Atlantic Ocean. The last two panels are for April-June (AMJ) and June-August (JJA), or early and mid-summer of year (+1), respectively, when the cumulative effects of surface flux anomalies become evident in the warm pool characteristics.

The composite *WP* and *wp* evolutions differ considerably in both the Pacific and the Atlantic. The entire *WP* sequence shows stronger development in the Pacific, with the positive cold tongue anomaly being more extensive, more intense, and with positive values lasting well into the summer of the (+1) year. This sequence has SST anomalies between +0.5 °C and +1°C throughout most of the tropical Atlantic, from JFMA through JJA, with the strongest during AMJ. The largest Atlantic *WP* anomalies (1°C) begin off West Africa in JFMA and extend all the way to the Caribbean by AMJ. During AMJ the anomalous SST of the lingering El Niño in the ENP region west of Central America is significant, hence both the ENP and IAS portions of the warm pool

have been enhanced: the ENP directly, through Pacific Ocean dynamics such as Rossby and coastal Kelvin waves, and the IAS indirectly, through the atmospheric bridge (section 3).

The *wp* sequence, in contrast, shows the onset of post-El Niño cold anomalies in the eastern equatorial Pacific as early as AMJ, and by JJA the Pacific cold tongue is clearly colder than normal. By AMJ, SST has returned to normal in the ENP region off Central America and the Atlantic portion of the WHWP has not become anomalous. This means that during the JFMA period of Atlantic forcing, the heating anomaly in the Pacific has weakened considerably and that the conditions conducive to a well-developed anomaly of the divergent circulation do not exist. In the tropical Atlantic, SST anomalies are in the range of ±0.2°C throughout the *wp* sequence, with a predominance of small negative values north of the equator.

One prominent feature of the *WP* distributions should be noted. While SST is clearly above normal over the TNA region during JFMA and AMJ, it is below normal north of about 20°N during JFMA, extending into the Gulf of Mexico. This will be referred to later.

b. Surface flux forcing

Does the forcing by surface fluxes in the tropical Atlantic reflect the differences seen in Atlantic SSTA between the *WP* and *wp* groups of events? Figure 4 shows the *WP* (left) vs. *wp* (right) comparison for the net surface flux (Q_{NET}, upper panels) and the latent heat flux and short wave radiation components (Q_{LHF}, Q_{SWR}, lower panels). To demonstrate the degree of variability between flux data sets, the Q_{NET} for both the NCEP reanalysis and the ERA40 (Gibson et al. 1997) are shown, while for the components we show only the NCEP distributions. The period composited is JFMA,

shown by Klein et al. (1999) to be the critical period of strong forcing emanating from the Pacific anomaly. Flux anomalies are taken as positive corresponding to an oceanic heat gain.

The left-side panels (*WP*) clearly confirm the relationships shown by Enfield and Mayer (1997) and Klein et al. (1999). While the Pacific cold tongue is being cooled by surface fluxes in response to the strong positive SST anomaly there, the TNA is being strongly heated over the entire region between West Africa and Central America. Heating rates in the range of –25 to –60 Wm^{-2} and +25 to +50 Wm^{-2} are the norm for the Pacific and TNA, respectively. In effect, there has been a transfer of heat from the equatorial Pacific to the TNA, through the troposphere, during years of extensive warm pool development in the Atlantic.

The main difference between NCEP and ERA40 data for Q_{NET} is the smaller area of strong heat loss in the equatorial Pacific, shown in the NCEP reanalysis. The Atlantic shows very similar distributions for both reanalyses. In particular, note that both reanalyses show a strong heat loss in the Gulf of Mexico and western North Atlantic north of about 20°N, which corresponds well to the contemporaneous (JFMA) negative SST anomalies seen in Figure 3. The Gulf of Mexico cooling is expected during El Niño winters because of the southward-displaced storm track over the southern tier states and Gulf coast region (Compo and Sardeshmukh 2004; Compo et al. 2001). Notice also that both indicate a strong warming in the high-latitude North Atlantic north of about 40°N, and that taken together, the North Atlantic anomalies conform to a familiar tripole pattern (Marshall et al. 2001). We will take this up again in our discussion of possible NAO effects.

Both component flux terms show a contribution to the TNA heating for the *WP* group of events: about 15-35 Wm^{-2} from reduced evaporation (Q_{LHF}) and 10-15 Wm^{-2} from increased insolation (Q_{SWR}). The Q_{SWR} contribution has about half the intensity of the Q_{LHF} anomaly and covers a more limited area east of Venezuela that overlaps with the southern fringe of the Q_{LHF} area. This is consistent with the relative importance of these fluxes as described by Klein et al. (1999) for the Atlantic sector. In comparison with Q_{LHF} and Q_{SWR} , the amplitudes of longwave and sensible heat flux anomalies are smaller (not shown).

The *wp* group shows a very different picture for the fluxes (Figure 4, right side). While a coherent positive spatial pattern of net flux still covers most of the TNA region, the heating is much less intense, the same being true of the component flux anomalies. This probably reflects a lack of month-to-month persistence in the atmospheric bridge forcing over the JFMA period.

c. Divergent circulation

We now focus on the tropospheric patterns that are responsible for the surface flux distributions of Figure 4. Figure 5 shows the NCEP distributions of anomalous velocity potential and divergent wind at 200 and 850 hPa and the anomalous vertical velocity at 500 hPa, all during the critical forcing period of JFMA. Similar distributions can be seen just before and after JFMA, but less intense (not shown). The ERA40 distributions are very similar to Figure 5 (not shown).

We first note that the anomalous patterns are similar for both the *WP* (left) and the *wp* (right) groups, but the latter being much weaker. Consistent with the surface flux composites, this may indicate a lack of persistence in the *wp* events because of a Pacific heating anomaly that has decayed earlier in the forcing sequence (Figure 3). In contrast,

the peak period of Pacific SST anomalies at the end of the onset year of *WP* El Niño episodes (Figure 3) induces a persistent anomalous Walker circulation response during the succeeding winter months, consisting of weakened uplift over the Indonesian sector and weakened subsidence over the eastern Pacific. Also as expected, the anomalies of the associated regional Hadley circulations extend northward into the subtropics of the winter (northern) hemisphere in the western Pacific and western Atlantic.

Insofar as the Atlantic sector development is concerned, there are two features of particular note. First, the anomalous upper tropospheric divergence over the eastern equatorial Pacific extends northeastward into the subtropical North Atlantic; and second, that an anomalous convergence forms over northeastern South America, weakening the normal monsoonal convection prevalent there during the boreal winter. Together these two features account for a weakening of the normal winter Hadley circulation that emanates from the South American convection northward into the subtropical North Atlantic (divergent wind vectors). The weakened convergence over the subtropical North Atlantic near 30°N results in reduced subsidence which is evidenced by the positive mid-tropospheric anomaly of vertical velocity there (500 hPa).

Figure 1d shows the Atlantic regional Hadley index of Wang (2004) superimposed on the SSTA time series for the TNA region. The Hadley cell index is defined by the 500-mb vertical velocity anomaly difference between the regions of 2.5°–7.5°S, 40°–20°W, and 25°–30°N, 40°–20°W. The Hadley index has a significant correlation of –0.38 with the Pacific NINO-3 SSTA index. The figure shows that the Hadley index for the Atlantic is consistently negative (weak Hadley cell) in association with a warm

TNA.

The impact of the weakened winter Hadley cell in the Atlantic sector can be seen for the *WP* composite in Figure 6. In early winter (DJF) but even more clearly in late winter (JFMA), an anomalous cyclonic surface circulation and low sea level pressure form in the subtropical North Atlantic under the reduced Hadley subsidence near 30°N. The associated southwesterly surface wind anomalies along 20°N are fully consistent with the reduced evaporative heat loss there and conform to the previous findings of Enfield & Mayer (1997) and others. By AMJ, when the SST anomalies have become fully established (Figure 2), the cyclonic pattern has disappeared. Note that in the *wp* composite the cyclonic anomaly is reduced and restricted to mid- and high latitudes, and that there is no weakening of the NE trades near 20°N.

To summarize, the *WP* and *wp* composite evolutions do indeed support the notion that the nature of the El Niño anomaly in the Pacific is related to the establishment (or not) of an atmospheric bridge from the Pacific to the Atlantic and a related large warm pool. As we shall see, however, other factors can influence the bridge and/or its effectiveness and that the El Niño events of the last 50 years cannot be cleanly categorized into the binary possibilities of bridge or no-bridge.

5. Influences other than the atmospheric bridge

Besides the remote forcing from the Pacific to the Atlantic, several additional factors can potentially influence the development of large warm pools.

a. Eastern North Pacific SST anomalies

The first, and most obvious factor is that if the El Niño in the easternmost, low-latitude Pacific persists into the summer of the second (+1) year, the ENP portion of the

warm pool can be larger and thus can result in a larger than normal WHWP regardless of the existence (or not) of a teleconnection into the Atlantic. ENP developments do not involve that teleconnection process; rather, they depend on how the low-latidude eastern Pacific anomalies evolve during an El Niño event in response to ocean-atmosphere interactions farther west. They are important, however, because they affect the total warm pool size (Figure 1a) seen by the atmosphere.

In Figure 7 we show the biennial evolutions of the NINO 1+2 index (80-90°W, 0-10°S) for the *WP* (upper panel) and *wp* (lower panel) events. In the upper panel we can see that all the *WP* events had positive eastern Pacific SST anomalies of one degree or more at least until July (+1). Of the *wp* events, however, only 1992 had significant persistence into the March-May period (+1). This clearly suggests that the warm pool in the Pacific did not have enough persistence through the late winter and early spring of most *wp* events to energize the atmospheric bridge. But it also signals that at least part of the warm pool anomaly of WP events can be due to the warmth of the ENP region after May (+1), in addition to or in lieu of an Atlantic anomaly.

b. North Atlantic oscillation

Boreal winter climate variability in the North Atlantic is embodied by the North Atlantic Oscillation (NAO) and is mostly independent of El Niño-Southern Oscillation (ENSO). The NAO is characterized by low-level atmospheric pressure (SLPA) nodes near southern Greenland (mean SLP low) and the eastern subtropical Atlantic (mean SLP high) (Marshall et al. 2001). When the pressure of the former is higher than normal and that of the latter is lower, the NAO is said to be in its negative phase and the westerly winds between the nodes are weaker than normal. The SSTA signature of the NAO is a tripole pattern which for positive NAO is cool in a broad region south of

Greenland, cool in the TNA and somewhat warm between those nodes, off the east coast of the United States (Marshall et al. 2001). This pattern is induced by stronger westerlies in the mid-to-high latitudes of the North Atlantic and stronger easterlies in the TNA region, both consonant with a stronger subtropical high pressure system. The correlation of winter seasonal anomalies (January-February-March) of the Lisbon-Reykjavik index of the NAO versus those of the NINO 3.4 index for the equatorial Pacific is maximum at zero lag but insignificant (-0.18). Hence, the interannual fluctuations of the NAO can randomly interfere with or reinforce the atmospheric bridge forcing from the Pacific during the winter months when both patterns are active (e.g., Mo and Hakkinen 2001). Thus, when the winter NAO is positive it would tend to interfere with the development of the bridge from the Pacific, and vice-versa.

c. Tropical Atlantic variability (TAV)

It is possible that the TNA, in addition to being affected by the NAO, can be affected by SSTAs south of the Intertropical Convergence Zone (ITCZ), principally in the tropical South Atlantic (TSA). Statistically this is not an ubiquitous occurrence and is more likely to occur at decadal time scales than interannually (Enfield et al. 1999). However, modeling studies suggest that a warm anomaly south of the equator (TSA) can lead to a negative anomaly north of the equator (TNA) and vice versa through a process of wind-evaporation-SST feedback (WES, Carton et al. 1996; Chang et al. 1997). More recently, Giannini et al. (2004) have used an atmospheric GCM with observations to argue that winter preconditioning of the tropical Atlantic through WES-type interactions can indeed influence the outcome of the teleconnection from the Pacific.

d. Comparison of individual El Niño episodes

All of the four factors discussed above (bridge, ENP, NAO and TAV) can be perceived in one way or another by examining the nine El Niño events shown in Figure 1a, for the AMJ season. In Figure 8 we show a nine-map plot of the Pacific-Atlantic SSTA distributions with the five *WP* events (1958, 1969, 1983, 1987, 1998) arranged along the left and the bottom and the four *wp* events (1966, 1973, 1977, 1992) in the 2x2 group in the upper right quadrant. All five *WP* events have some enhancement of the Atlantic portion of the WHWP, with 1958 and 1969 being the strongest; all but 1987 have significant persistence of ENP anomalies north of 5°N in the eastern Pacific. Clearly the atmospheric teleconnection to the Atlantic is ubiquitous, but the persistence of SST anomalies in the ENP region is also a major contributor to warm pool development. Three of the *wp* events had returned to cool conditions in the equatorial Pacific and there is no sign of anomalous warmth in the Atlantic, while the ENP is also normal or cool. 1966 is somewhat equivocal because the ENP remains warm during MAM (+1) (see Figure 7) while the eastern TNA is warm and the size of the total warm pool is normal (Figure 1a). Finally, we again note the outlier case in which the equatorial Pacific was still warm in the spring of 1992, yet there was no warming in the Atlantic.

Figure 9 shows a similar nine-panel plot of the anomalous 200 hPa divergent circulation during the FMA period immediately preceding the SSTA maps of Figure 8. The maps for the *WP* years show a weakened regional Hadley circulation between northeastern South America (or eastern equatorial Atlantic) and the subtropical North Atlantic. In the case of the strong El Niños of 1982-83 and 1997-98 the anomalies are

especially strong and are part of a drastically altered divergent circulation around the globe. The *wp* events of 1973 and 1977 clearly lack this feature while 1966 shows a reduced convection over South America but the opposite convergence over Mexico does not extend into the subtropical North Atlantic, presumably required to affect the North Atlantic subtropical high pressure system.

The one outlier year that does not fit the *WP/wp* dichotomy is 1992. That year is somewhat opposite to 1966 in that the convergence (reduced convection) over South America is weak, but the pattern of divergence extending from the eastern North Pacific into the suptropical North Atlantic is clearly present, similar to 1983 and 1998 but not as intense. Hence, in the upper troposphere the forcing appears to have been favorable for producing a large warm pool. Yet, the TNA region was slightly cool (Figure 8) and the warm pool was close to normal (Figure 1a).

The 925 hPa geopotential height and wind anomalies in Figure 10 illustrate the extent to which the NAO might have played a role in two of the nine events. In AMJ of 1958 and 1969 the SST anomalies and warm pool contours (Figure 8) show that the western Pacific warm pool was only weakly anomalous compared with the strong El Niños of 1982-83 and 1997-98 when the warm pool extended much farther east. The anomalous divergent circulation, though favorable for the atmospheric bridge, was also much weaker (Figure 9). Yet, the 925 hPa anomalies were quite strong in the North Atlantic and correspond to a strongly negative NAO pattern, while the SST anomalies in the TNA region are stronger and more extensive than in 1983 and 1998. Hence, these two years are a good example of how the NAO pattern can reinforce the atmospheric bridge in the Pacific and produce a remarkable enhancement of the Atlantic warm pool.

Six other events — 1966, 1973, 1977, 1983, 1987, 1998 — show no NAO influence of either polarity. The patterns are spatially inconsistent with the canonical pattern of the NAO, as indicated by the positions of the Azores and Iceland, and the wind anomalies in the TNA region are not consistent with the kind of forcing seen in 1958 and 1969.

The outlier year — 1992 — shows evidence of interference by the NAO. That year is enigmatic, as it runs contrary to the logic of the atmospheric bridge. The large Indo-Pacific warm pool persisted into the spring of 1992 with strong SST anomalies in the eastern equatorial Pacific (Figure 7), and there was evidence of atmospheric bridge development in the Atlantic sector (Figure 9). Yet the TNA had weak-to-moderate negative SST anomalies during AMJ. Figure 10 shows a negative NAO pattern with stronger than normal low-level easterly flow over the TNA region, suggesting that the surface high pressure system was not weakened by the weak upper tropospheric subsidence over the subtropical North Atlantic.

Finally, we note that only one year — 1958 — had a strong dipole distribution of SSTA straddling the ITCZ in the tropical Atlantic, suggestive of a wind-evaporation-SST feedback between the tropical North Atlantic (TNA) and South Atlantic (TSA). However, considering the strong combination of atmospheric bridge plus the negative NAO of that winter, both favorable for TNA warming, it seems more likely that the TNA anomaly forced the TSA region, rather than vice-versa. This is also consistent with the analysis of (Enfield et al. 1999) who show statistically that TNA forcing of TSA is more probable than the reverse.

6. Discussion and conclusions

Our analysis has verified that the nature of the Pacific El Niño can affect the development (or not) of a teleconnection to the tropical North Atlantic. The primary factor, however, appears to be the persistence of Pacific anomalies rather than their intensity overall. The suggestion from the composite analysis (section 4) that the intensity of the Pacific El Niño plays a role in energizing the atmospheric bridge is borne out neither by Figure 7 nor by the examination of individual events (section 5d); El Niño events of all intensities result in Atlantic teleconnections. Three of the events that produced large warm pools (1957-58, 1968-69, 1986-87) had eastern Pacific anomalies of less than 1.5°C at the end of the onset year when the atmospheric bridge typically begins to be forced, whilst one strong event with SSTA over 2°C (1972-73) did not produce a large warm pool. Except for the enigmatic case of 1992, which was apparently interfered with by the NAO, the critical factor seems to be whether or not significant SST anomalies in the Pacific persist into the boreal spring months of the following year (Figure 7). These conclusions do not depend on which Pacific SSTA index is examined.

Our search for Atlantic sector phenomena that may independently influence atmospheric bridge development reveals that in two of the nine events (1958 and 1969) a strong boreal winter, negative NAO pattern reinforced the signal from the Pacific to produce extraordinarily large warm pools. One clear instance of interference by a positive NAO pattern was found for 1992, which otherwise would probably have had a large warm pool that summer. Finally, no clear evidence could be found that tropical Atlantic variability (TAV) modified the teleconnection from the Pacific, but we cannot

categorically discard the possibility that the 1958 warm pool was partly enhanced by a favorable WES feedback.

We have shown that extraordinarily large Western Hemisphere warm pools occur following El Niño events in the Pacific, but that this only happens about half of the time, not consistently enough to make the fact of an El Niño the basis for anticipating a large warm pool. However, the knowledge gained here can be used to form a strategy for predicting large warm pools 1-2 seasons in advance of the summer following El Niño events. Two factors must be monitored during the winter through early spring: the persistence of the SST anomalies in the Pacific and the presence of a significant positive or negative NAO pattern in the North Atlantic. If the Indo-Pacific warm pool remains anomalous into the early months of the year and eastern Pacific SST anomalies persist well past February, the ENP portion of the warm pool will be large and the atmospheric bridge to the Atlantic will likely be active, both favoring a large WHWP if no mitigating NAO pattern exists. If a negative NAO pattern develops, typically between December and March, it is highly likely that a strong warm pool will develop as in 1958 and 1969, even if the Pacific El Niño event is not strong. If a positive NAO pattern develops, this will likely mitigate against having a large Atlantic warm pool, as occurred in 1992.

The ability of present coupled models to help in the prediction of large warm pools is limited. As shown by Landsea and Knaff (2000), the skill of these models in predicting either the intensity or the timing of onset and decay of El Niño events is quite poor. However, it is possible that some of the models may have enough skill at short lead times that they may be used to predict SSTA persistence in the Pacific during

the critical MAM (+1) period if they are initialized at the end of the onset year. On the other hand, we know of no models that can predict the evolution of the teleconnection to the Atlantic, nor the future state of the NAO. Hence, for the foreseeable future the best hope for warm pool prediction is to monitor Pacific SSTA and the NAO in the Atlantic, using the global observation system.

In reference to Figure 1 we showed that, unlike the year following El Niño, the El Niño onset years show no clear tendency toward having large Atlantic warm pools. A fair question is, if El Niño-induced warm pool anomalies are not favored during the onset year, why is a developing El Niño in the Pacific associated with fewer hurricanes in the Atlantic (Gray 1984; Landsea 2000). The answer, we feel, is that the Atlantic Ocean is not involved in mediating the teleconnection to Atlantic hurricanes during the onset year. As the Indo-Pacific warm pool anomaly grows into the summer of the onset year, the tropical atmosphere immediately transmits upper-level zonal wind anomalies into the Atlantic sector, most likely through atmospheric Kelvin wave propagation. This increases the upper-tropospheric wind shear in the Atlantic, which in turn discourages hurricane development. In fact, other meteorological anomalies also occur in the western hemisphere during the June-October period of the onset year for similar reasons (Ropelewski and Halpert 1987). However, even if the Atlantic surface winds were also affected, modification of the ocean surface heat budget in the Atlantic requires a 1-2 season delay, by which time the Atlantic warm pool season has ended.

Acknowledgments. This work was supported by the National Oceanic and Atmospheric Administration (NOAA) CLIVAR-PACS program grant number GC03-114 and by the base funding of the Atlantic Oceanographic and Meteorological Laboratory. We wish

to thank Dr. Chris Landsea who reviewed the manuscript prior to submission, as well as the anonymous reviewers consulted by the *Journal of Climate*.

References

Carton, J. A., X. H. Cao, B. S. Giese, and A. M. da Silva, 1996: Decadal and interannual SST variability in the tropical Atlantic Ocean. *J. Phys. Oceanogr.*, **26,** 1165-1175.

Chang, P., L. Ji, and H. Li, 1997: A decadal climate variation in the tropical Atlantic Ocean from thermodynamic air-sea interactions. *Nature*, **385,** 516-518.

Compo, G. P. and P. D. Sardeshmukh, 2004: Storm Track predictability on seasonal and decadal scales. *J. Climate*, **17,** 3701-3720.

Compo, G. P., P. D. Sardeshmukh, and C. Penland, 2001: Changes of subseasonal variability associated with El Niño. *J. Climate*, **14,** 3356-3374.

Enfield, D. B., 1989: El Niño, past and present. *Reviews of Geophysics*, **27,** 159-187.

——, 1996: Relationships of inter-American rainfall to tropical Atlantic and Pacific SST variability. *Geophysical Research Letters*, **23,** 3305-3308.

Enfield, D. B. and D. A. Mayer, 1997: Tropical Atlantic sea surface temperature variability and its relation to El Niño-Southern Oscillation. *Journal of Geophysical Research*, **102,** 929-945.

Enfield, D. B., A. M. Mestas-Nuñez, D. A. Mayer, and L. Cid-Serrano, 1999: How ubiquitous is the dipole relationship in tropical Atlantic sea surface temperatures? *Journal of Geophysical Research*, **104,** 7841-7848.

Giannini, A., R. Saravanan, and P. Chang, 2004: The preconditioning role of tropical Atlantic variability in the development of the ENSO teleconnection: implications for the prediction of Nordeste rainfall. *Climate Dynamics*, **22,** 839-855.

Gibson, J. K., P. Kållberg, S. Uppala, A. Hernandez, A. Nomura, and E. Serrano, 1997: ERA description. Re-Analysis (ERA) Project Report Series No. 1, 72 pp.

Gray, W. M., 1984: Atlantic seasonal hurricane frequency, Part II: Forecasting its variability. *Monthly Weather Review*, **112,** 1669-1683.

Hastenrath, S., 1979: On modes of tropical circulation and climate anomalies. *J. Atmos. Sci.*, **35,** 2222-2231.

——, 2000: Upper air mechanisms of the Southern Oscillation in the tropical Atlantic sector. *J. Geophys. Research*, **105,** 14997-15009.

Hoskins, B. J. and K. Karoly, 1981: The steady response of a spherical atmosphere to thermal and orographic forcing. *J. Atmos. Sci.*, **38,** 1179-1196.

Hurrell, J. W., 1995: Decadal trends in the North Atlantic Oscillation, 1995: Regional temperatures and precipitation. *Science*, **269,** 676-679.

Kalnay, E., M. Kanamitsu, R. Kistler, W. Collins, D. Deaven, L. Gandin, M. Iredell, S. Saha, G. White, J. Woollen, Y. Zhu, M. Chelliah, W. Ebisuzaki, W. Higgins, J. Janowiak, K. C. Mo, C. Ropelewski, J. Wang, Leetmaa, R. Reynolds, R. Jenne, and D. Joseph, 1996: The NCEP/NCAR 40-year Reanalysis Project. *Bulletin of the American Meteorological Society*, **77,** 437-471.

Klein, S. A., B. J. Soden, and N. C. Lau, 1999: Remote sea surface temperature variations during ENSO: Evidence for a tropical Atmospheric bridge. *Journal of Climate*, **12,** 917-932.

Landsea, C., 2000: El Nio-Southern Oscillation and the seasonal variability of tropical cyclones. *Impact of Multiscale Variability on Natural Ecosystems and Society*, A. Diaz and V. Markgraf, Eds., Cambridge University Press, 149-181.

Landsea, C. W. and J. A. Knaff, 2000: How Much Skill Was There in Forecasting the Very Strong 1997-98 El Niño? *Bulletin of the American Meteorological Society*, **81,** 2107-2120.

Marshall, J., Y. Kushnir, D. Battisti, P. Chang, A. Czaja, R. Dickson, J. Hurrell, M. McCartney, R. Saravanan, and M. Visbeck, 2001: North Atlantic Climate Variability: Phenomena, Impacts And Mechanisms. *International Journal of Climatology*, **21,** 1863–1898.

Mo, K. C. and S. Hakkinen, 2001: Interannual Variability in the Tropical Atlantic and Linkages to the Pacific. *Journal of Climate*, **14,** 2740-2762.

Quinn, W. H. and V. T. Neal, 1992: The historical record of El Nino events. *Climate Since A.D. 1500*, R. S. Bradley and P. D. Jones, Eds., Routledge.

Quinn, W. H., V. T. Neal, and S. A. d. Mayolo, 1987: El Niño occurrences over the past four and a half centuries. *Journal of Geophysical Research*, **92,** 14,449-14,461.

Rasmusson, E. M. and T. H. Carpenter, 1982: Variations in tropical sea surface temperature and surface wind fields associated with the Southern Oscillation/El Niño. *Monthly Weather Review*, **110,** 354-384.

Ropelewski, C. F. and M. S. Halpert, 1987: Global and regional scale precipitation patterns associated with the El Niño/Southern Oscillation. *Monthly Weather Review*, **115,** 1606-1626.

Smith, T. M., R. W. Reynolds, R. E. Livezey, and D. C. Stokes, 1996: Reconstruction of Historical Sea Surface Temperatures Using Empirical Orthogonal Functions. *Journal of Climate*, **9,** 1403-1420.

Wallace, J. M. and D. S. Gutzler, 1981: Teleconnections in the geopotential height field during the northern hemisphere winter. *Monthly Weather Review*, **109,** 784-812.

Wang, C., 2004: ENSO, Atlantic climate variability, and the Walker and Hadley circulations. *The Hadley Circulation: Present, Past, and Future*, A. Diaz and R. S. Bradley, Eds., Cambridge University Press, in press.

Wang, C. and D. B. Enfield, 2001: The Tropical Western Hemisphere warm pool. *Geophysical Research Letters*, **28,** 1635-1638.

——, 2003: A further study of the tropical Western Hemisphere warm pool. *Journal of Climate*, **16,** 1476-1493.

Figure captions

Figure 1. (a) Time series of the total Western Hemisphere warm pool (WHWP) area index, defined as the anomaly of the area surrounded by the 28.5°C isotherm of sea surface temperature (SST), expressed as a percentage of the average July value. (b) As in (a) but for the eastern North Pacific (ENP) only, expressed as a percentage of the average May value. (c) As in (a) but for the intra-Americas Sea (IAS) only, expressed as a percentage of the average September value. (d) Anomaly of sea surface temperature averaged over the tropical North Atlantic (solid) superimposed with the Atlantic Hadley index of Wang (2004). Years of El Niño onset (0) and decay (+1) are indicated by vertical hash marks in panel (a).

Figure 2. (a) Climatological boreal winter (December-January-February) velocity potential and divergent wind at 200 hPa from the NCAR/NCEP reanalysis (Kalnay et al. 1996). (b) As in (a) but for anomalies composited for El Niño winters. (c) Anomalies of 500 hPa vertical velocity composited for El Niño winters. Positive anomalies of vertical velocity near 25-30°N in the Atlantic indicate reduced subsidence and negative values over northern South America indicate reduced convection.

Figure 3. Left panels: seasonal evolution of the global distribution of sea surface temperature anomaly (shading) from boreal winter (DJF) to summer (JJA), averaged for five Niño +1 years with extraordinarily large warm pools (Figure 1a) and superimposed with the climatological average isotherms (27.5°C, 27.0°C and 28.5°C, solid contours) that define the tropical warm pools. Right Panels: as on the left, but for four Niño +1 years in which large Atlantic warm pools did not develop (Figure 1a).

Figure 4. Left panels: global distribution of late winter to early spring (JFMA) heat flux anomaly (shading) averaged for five Niño +1 years with extraordinarily large warm pools (Figure 1). Net surface heat flux (Q_{NET}) from the NCEP and ERA40 reanalyses is shown above the color bar; latent heat flux (Q_{LHF}) and shortwave radiation (Q_{SWR}) are shown below. Right panels: as on the left, but for four Niño +1 years in which large Atlantic warm pools did not develop (Figure 1).

Figure 5. Left panels: from top to bottom, the January-April (JFMA) composite anomalies of velocity potential (shading) and divergent wind (vectors) at 850 hPa and 200 hPa levels of the troposphere, and the vertical velocity (shading) at 500 hPa, averaged for five Niño +1 years with extraordinarily large warm pools (Figure 1). Right panels: as on the left, but for four Niño +1 years in which large Atlantic warm pools did not develop (Figure 1).

Figure 6. Left panels: seasonal evolution of the global distribution of anomalous sea level pressure (shading and contours) and surface wind (vectors) averaged for five Niño +1 years with extraordinarily large warm pools (Figure 1). Right Panels: as on the left, but for four Niño +1 years in which large Atlantic warm pools did not develop (Figure 1).

Figure 7. Upper panel: Two-year evolution of Pacific El Niño events in the eastern equatorial Pacific (NINO 1+2 index) for five El Niños followed by large warm pools. Lower Panel: As above, but for four Niño +1 years in which large Atlantic warm pools did not develop (Figure 1).

Figure 8. Left and bottom panels: Sea surface temperature anomaly (shading) and climatological warm pool isotherms (contours) for the April-May-June period of (+1) years with large warm pools following El Niño. Upper-right panels highlighted by rectangle: SST anomaly for four Niño +1 years in which large Atlantic warm pools did not develop (see discussion of Figure 1).

Figure 9. Left and bottom panels: Anomaly of velocity potential and divergent wind at 200 hPa for the February-March-April period of (+1) years with large warm pools following El Niño. Upper-right panels highlighted by rectangle: Anomaly of velocity potential and divergent wind for four Niño +1 years in which large Atlantic warm pools did not develop (see discussion of Figure 1).

Figure 10. Left and bottom panels: Anomaly of geopotential height and wind at 925 hPa for the February-March-April period of (+1) years with large warm pools following El Niño. Upper-right panels highlighted by rectangle: Anomaly of geopotential height and wind for four Niño +1 years in which large Atlantic warm pools did not develop

(see discussion of Figure 1). The small white boxes represent the nominal centers of the NAO nodes in the Azores Islands and western Iceland.

Figure captions

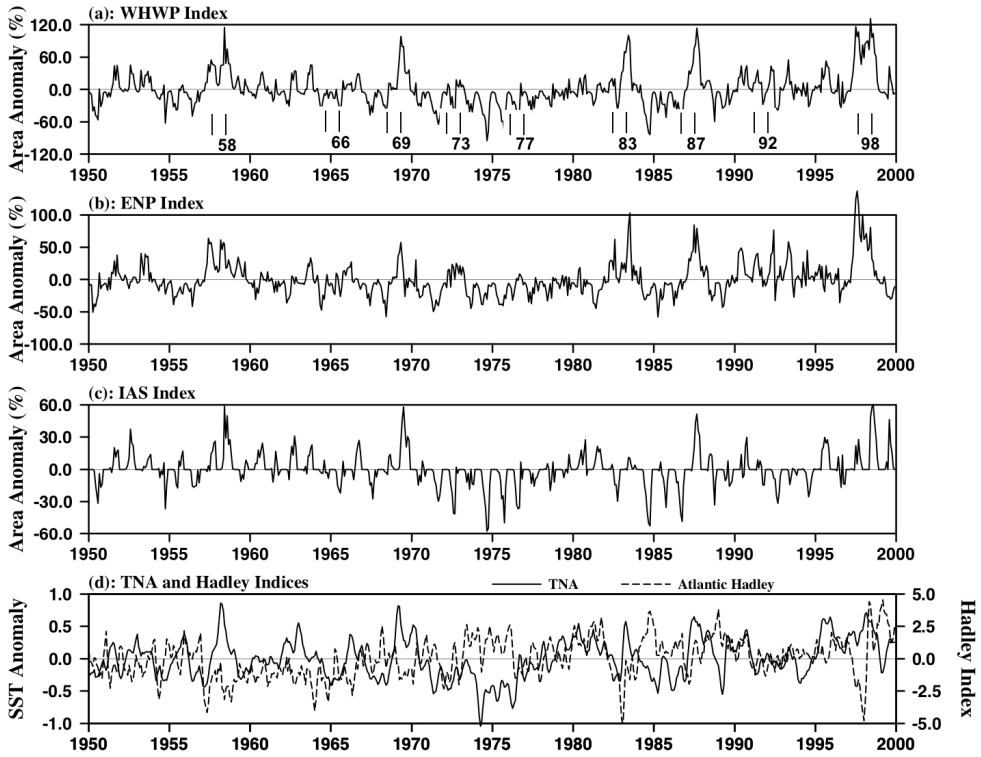

Figure 1. (a) Time series of the total Western Hemisphere warm pool (WHWP) area index, defined as the anomaly of the area surrounded by the 28.5°C isotherm of sea surface temperature (SST), expressed as a percentage of the average July value. (b) As in (a) but for the eastern North Pacific (ENP) only, expressed as a percentage of the average May value. (c) As in (a) but for the intra-Americas Sea (IAS) only, expressed as a percentage of the average September value. (d) Anomaly of sea surface temperature averaged over the tropical North Atlantic (solid) superimposed with the Atlantic Hadley index of Wang (2004). Years of El Niño onset (0) and decay (+1) are indicated by vertical hash marks in panel (a).

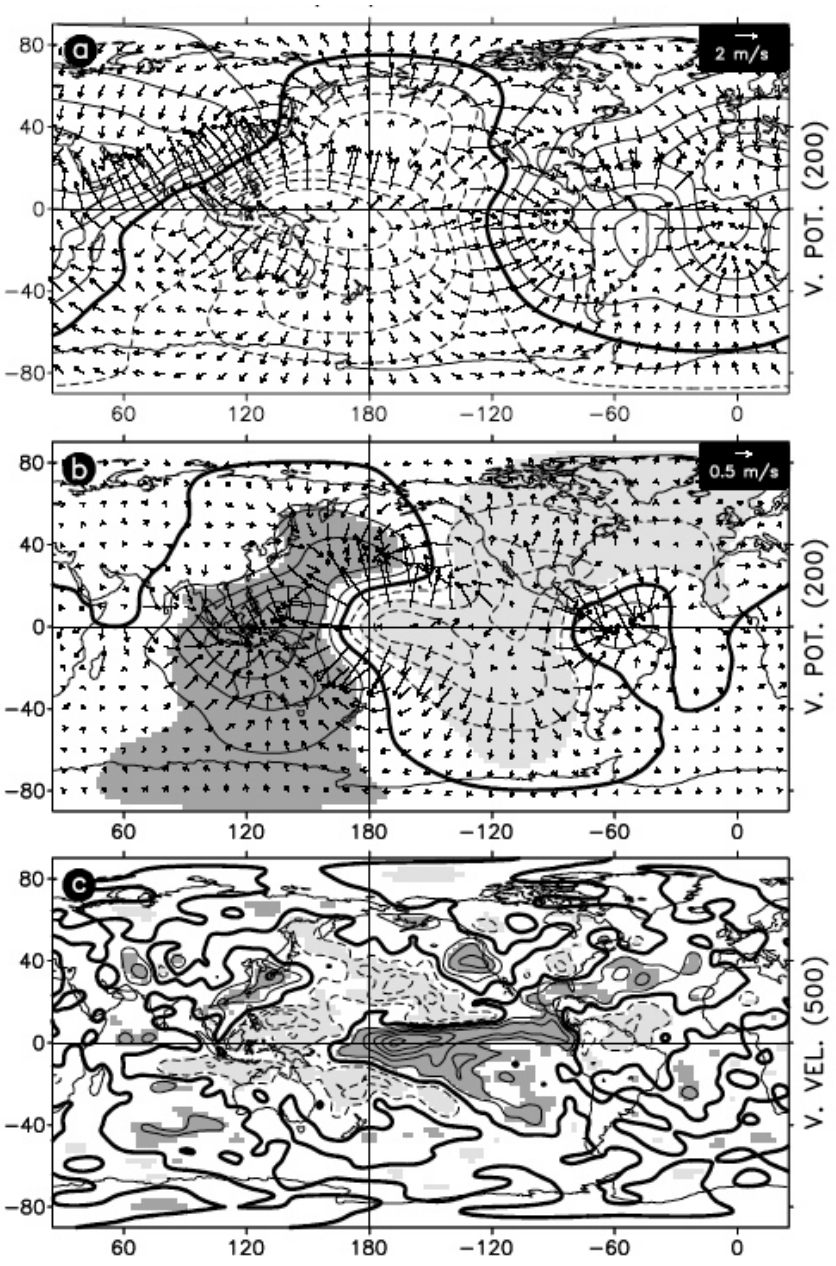

Figure 2. (a) Climatological boreal winter (December-January-February) velocity potential and divergent wind at 200 hPa from the NCAR/NCEP reanalysis (Kalnay et al. 1996). (b) As in (a) but for anomalies composited for El Niño winters. (c) Anomalies of 500 hPa vertical velocity composited for El Niño winters. Positive anomalies of vertical velocity near 25-30°N in the Atlantic indicate reduced subsidence and negative values over northern South America indicate reduced convection.

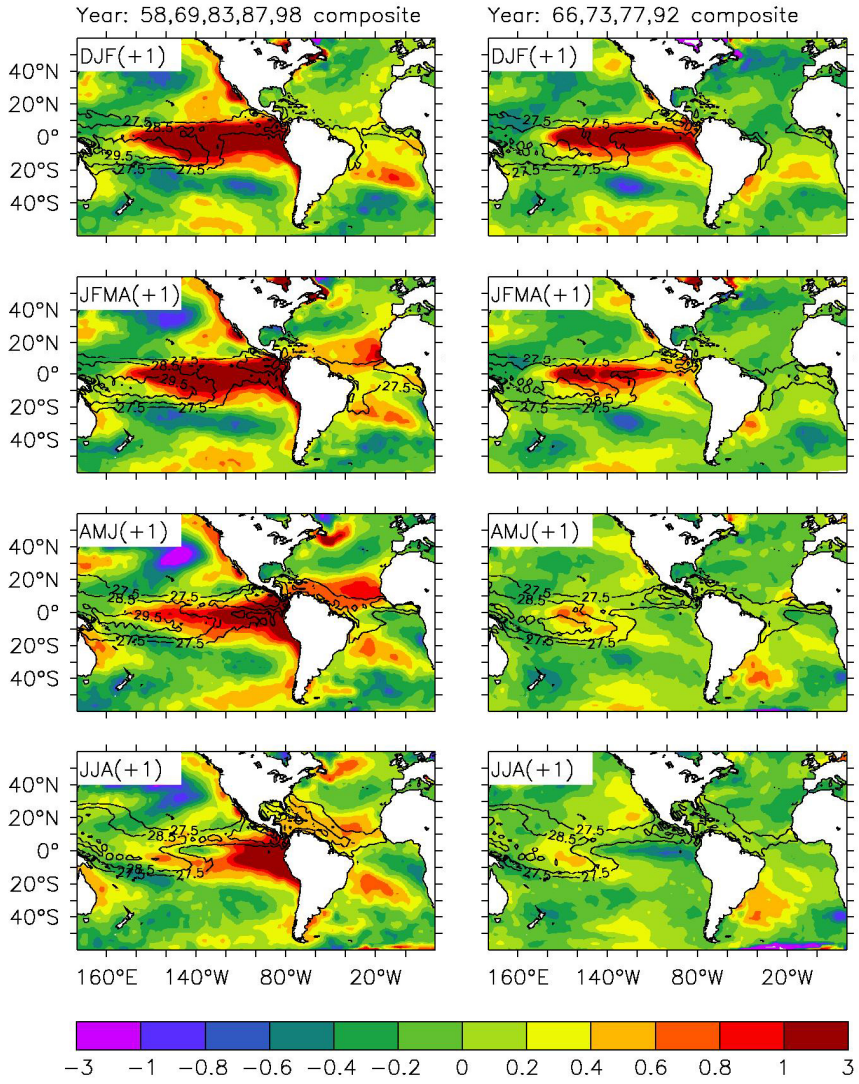

Figure 3. Left panels: seasonal evolution of the global distribution of sea surface temperature anomaly (shading) from boreal winter (DJF) to summer (JJA), averaged for five Niño +1 years with extraordinarily large warm pools (Figure 1a) and superimposed with the actual seasonally averaged isotherms (27.5°C, 27.0°C and 28.5°C, solid contours) that define the tropical warm pools. Right Panels: as on the left, but for four Niño +1 years in which large Atlantic warm pools did not develop (Figure 1a).

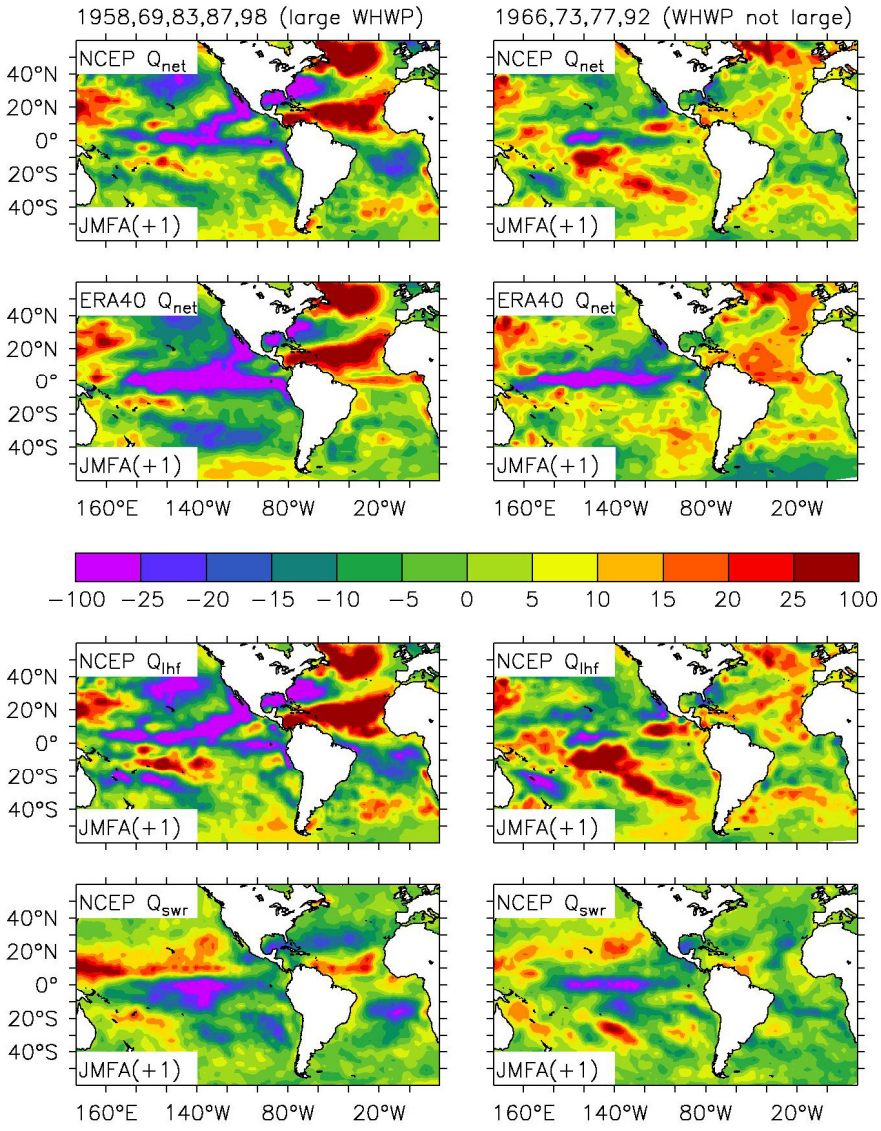

Figure 4. Left panels: global distribution of late winter to early spring (JFMA) heat flux anomaly (shading) averaged for five Niño +1 years with extraordinarily large warm pools (Figure 1). Net surface heat flux (Q_{NET}) from the NCEP and ERA40 reanalyses is shown above the color bar; latent heat flux (Q_{LHF}) and shortwave radiation (Q_{SWR}) are shown below. Right panels: as on the left, but for four Niño +1 years in which large Atlantic warm pools did not develop (Figure 1).

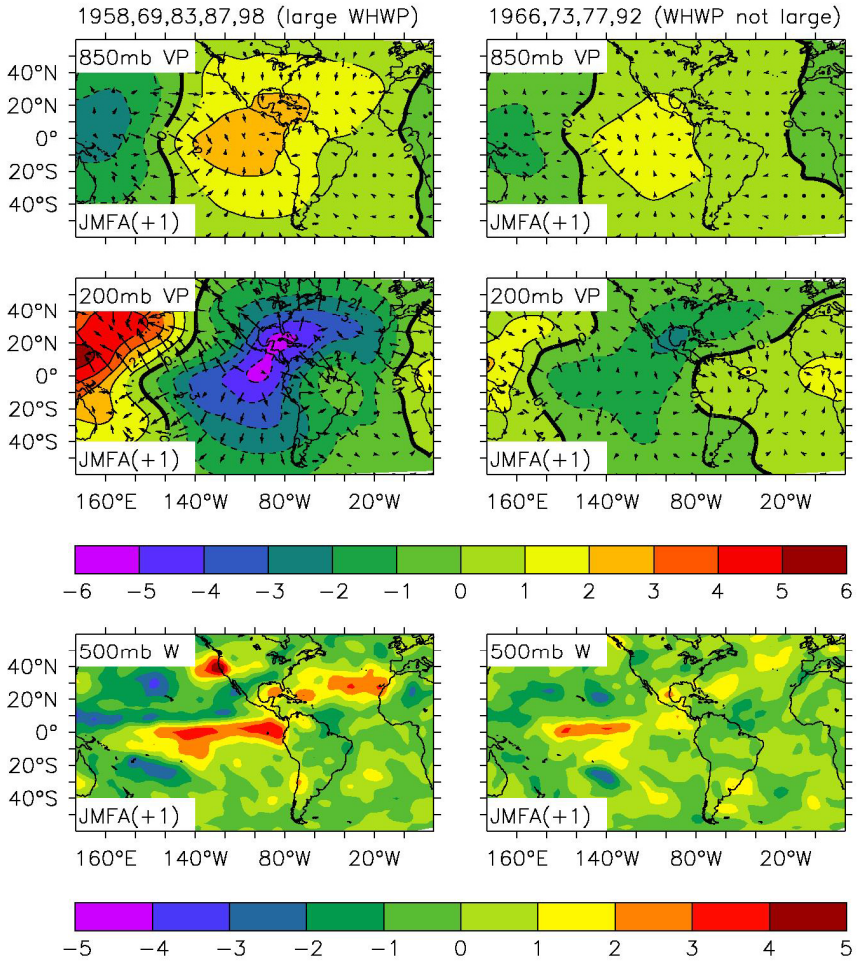

Figure 5. Left panels: from top to bottom, the January-April (JFMA) composite anomalies of velocity potential (shading) and divergent wind (vectors) at 850 hPa and 200 hPa levels of the troposphere, and the vertical velocity (shading) at 500 hPa, averaged for five Niño +1 years with extraordinarily large warm pools (Figure 1). Right panels: as on the left, but for four Niño +1 years in which large Atlantic warm pools did not develop (Figure 1).

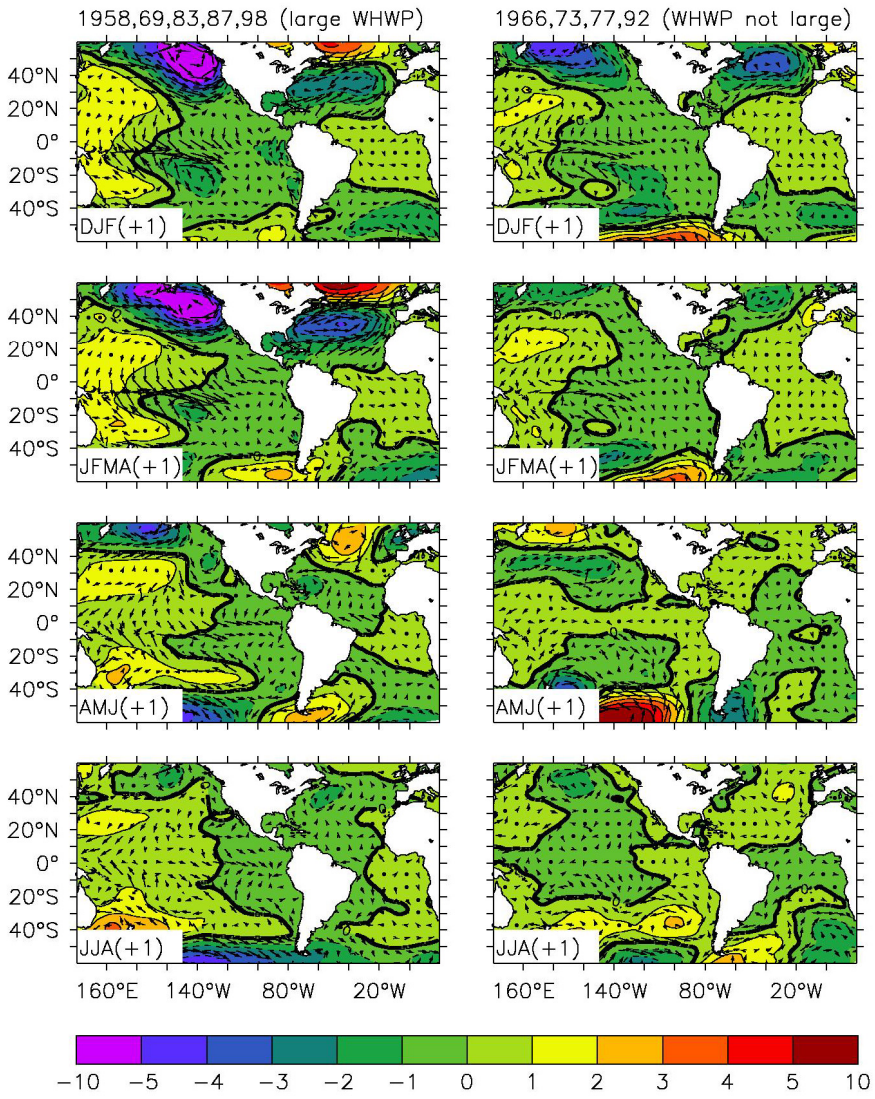

Figure 6. Left panels: seasonal evolution of the global distribution of anomalous sea level pressure (shading and contours) and surface wind (vectors) averaged for five Niño +1 years with extraordinarily large warm pools (Figure 1). Right Panels: as on the left, but for four Niño +1 years in which large Atlantic warm pools did not develop (Figure 1).

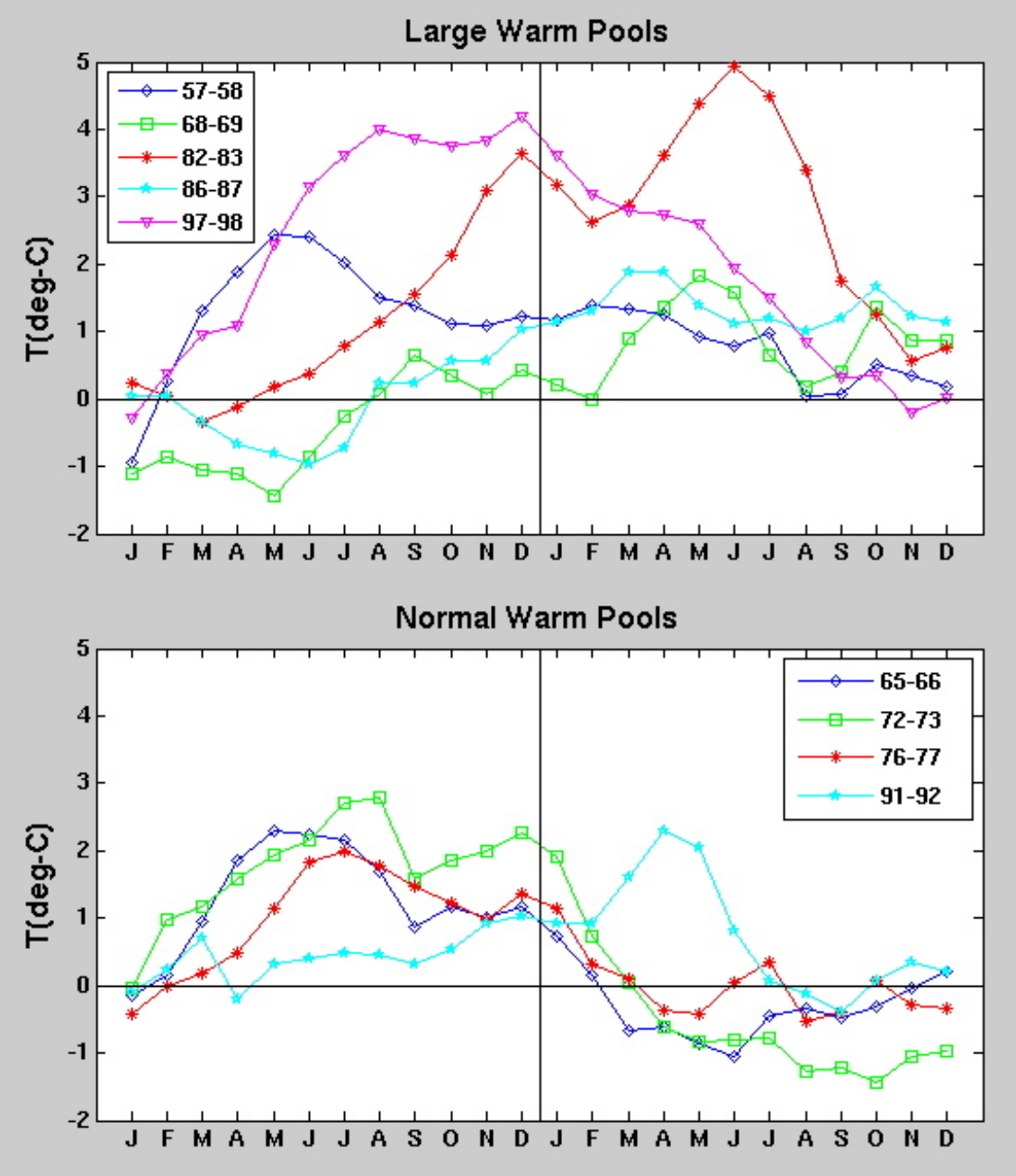

Figure 7. Upper panel: Two-year evolution of Pacific El Niño events in the eastern equatorial Pacific (NINO 1+2 index) for five El Niños followed by large warm pools. Lower Panel: As above, but for four Niño +1 years in which large Atlantic warm pools did not develop (Figure 1).

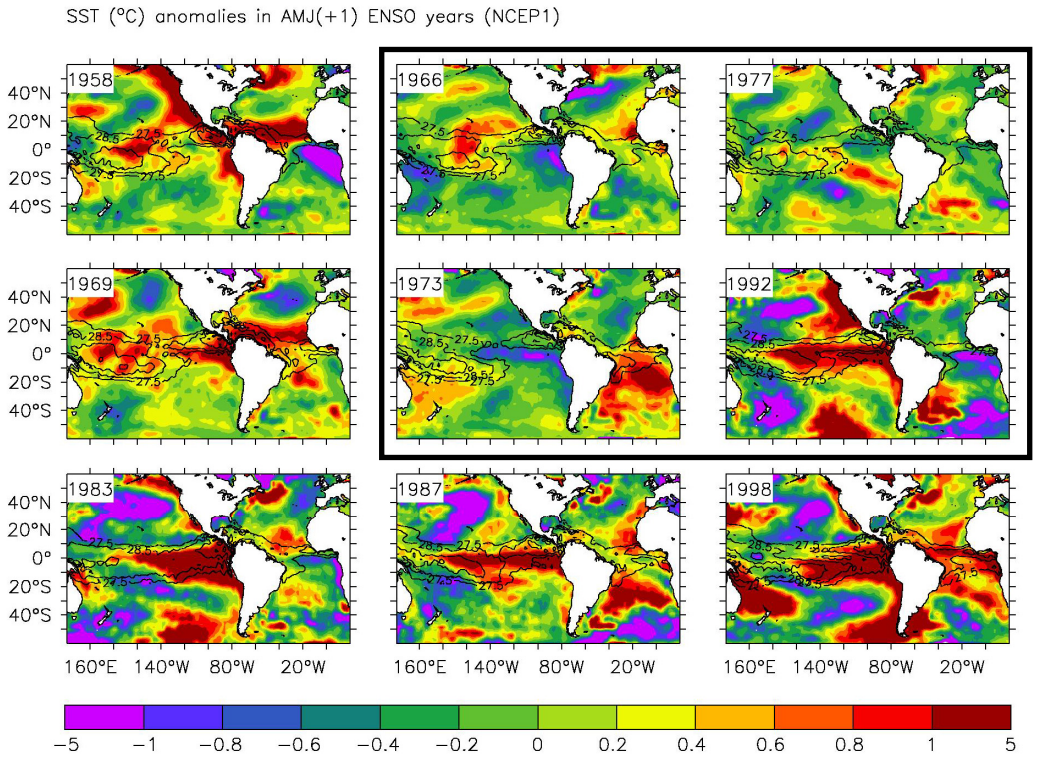

Figure 8. Left and bottom panels: Sea surface temperature anomaly (shading) and climatological warm pool isotherms (contours) for the April-May-June period of (+1) years with large warm pools following El Niño. Upper-right panels highlighted by rectangle: SST anomaly for four Niño +1 years in which large Atlantic warm pools did not develop (see discussion of Figure 1). The actual contours of the warm pools during the same years are shown superimposed.

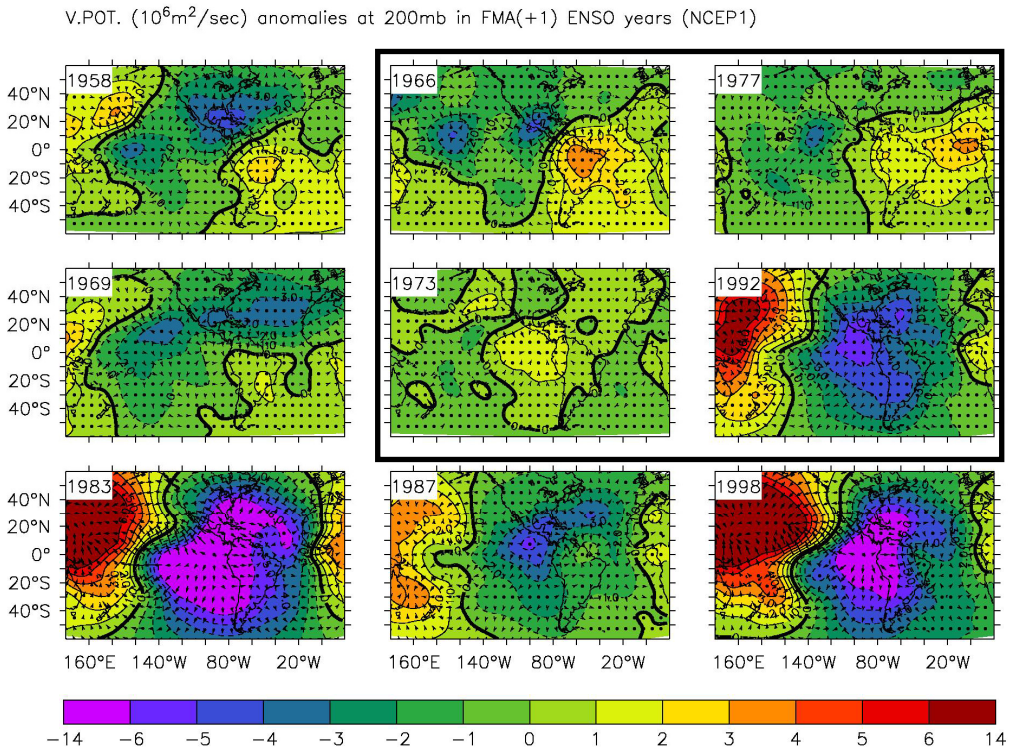

Figure 9. Left and bottom panels: Anomaly of velocity potential and divergent wind at 200 hPa for the February-March-April period of (+1) years with large warm pools following El Niño. Upper-right panels highlighted by rectangle: Anomaly of velocity potential and divergent wind for four Niño +1 years in which large Atlantic warm pools did not develop (see discussion of Figure 1).

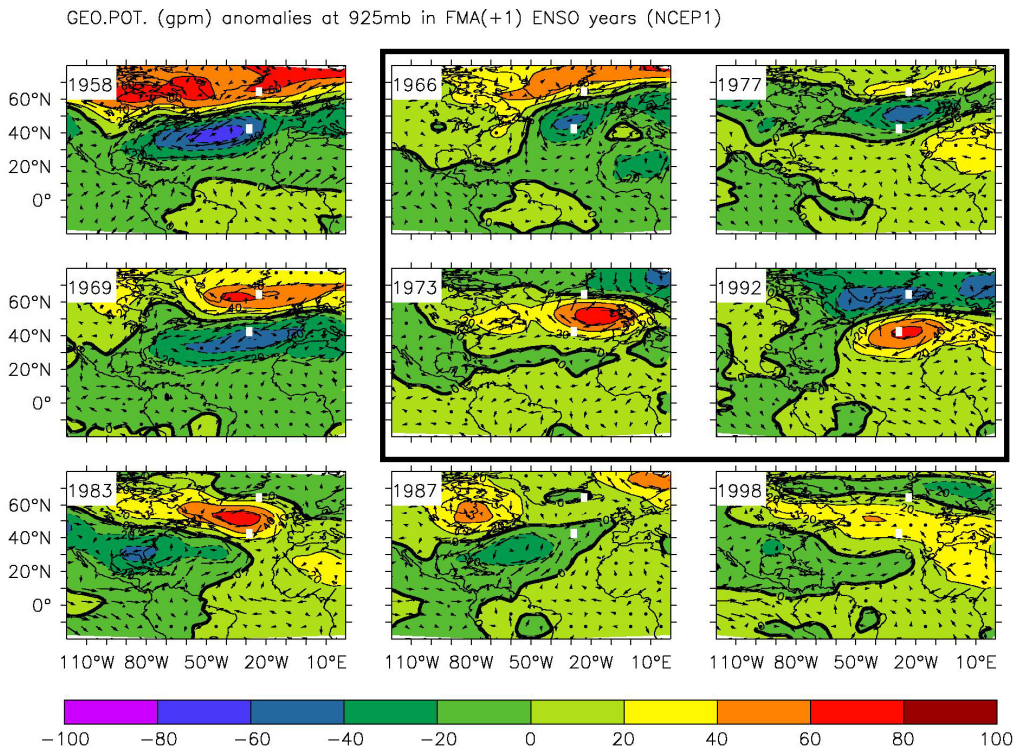

Figure 10. Left and bottom panels: Anomaly of geopotential height and wind at 925 hPa for the February-March-April period of (+1) years with large warm pools following El Niño. Upper-right panels highlighted by rectangle: Anomaly of geopotential height and wind for four Niño +1 years in which large Atlantic warm pools did not develop (see discussion of Figure 1). The small white boxes represent the nominal centers of the NAO nodes in the Azores Islands and western Iceland.